

Christian Iliadis

Nuclear Physics of Stars



WILEY-VCH Verlag GmbH & Co. KGaA

This Page Intentionally Left Blank

Christian Iliadis

Nuclear Physics of Stars

1807–2007 Knowledge for Generations

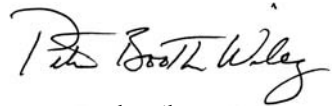
Each generation has its unique needs and aspirations. When Charles Wiley first opened his small printing shop in lower Manhattan in 1807, it was a generation of boundless potential searching for an identity. And we were there, helping to define a new American literary tradition. Over half a century later, in the midst of the Second Industrial Revolution, it was a generation focused on building the future. Once again, we were there, supplying the critical scientific, technical, and engineering knowledge that helped frame the world. Throughout the 20th Century, and into the new millennium, nations began to reach out beyond their own borders and a new international community was born. Wiley was there, expanding its operations around the world to enable a global exchange of ideas, opinions, and know-how.

For 200 years, Wiley has been an integral part of each generation's journey, enabling the flow of information and understanding necessary to meet their needs and fulfill their aspirations. Today, bold new technologies are changing the way we live and learn. Wiley will be there, providing you the must-have knowledge you need to imagine new worlds, new possibilities, and new opportunities.

Generations come and go, but you can always count on Wiley to provide you the knowledge you need, when and where you need it!



William J. Pesce
William J. Pesce
President and Chief Executive Officer



Peter Booth Wiley
Peter Booth Wiley
Chairman of the Board

Christian Iliadis

Nuclear Physics of Stars



WILEY-VCH Verlag GmbH & Co. KGaA

The Author

Prof. Christian Iliadis
University of North Carolina
at Chapel Hill
176, Phillips Hall
Chapel Hill, NC 27599-3255
USA

Cover illustration

by Roger Wagner

All books published by Wiley-VCH are carefully produced. Nevertheless, authors, editors, and publisher do not warrant the information contained in these books, including this book, to be free of errors. Readers are advised to keep in mind that statements, data, illustrations, procedural details or other items may inadvertently be inaccurate.

Library of Congress Card No.:
applied for

British Library Cataloguing-in-Publication Data

A catalogue record for this book is available from the British Library.

Bibliographic information published by the Deutsche Nationalbibliothek

Die Deutsche Nationalbibliothek lists this publication in the Deutsche Nationalbibliografie; detailed bibliographic data are available in the Internet at <<http://dnb.d-nb.de>>.

© 2007 WILEY-VCH Verlag GmbH & Co. KGaA, Weinheim

All rights reserved (including those of translation into other languages). No part of this book may be reproduced in any form – by photoprinting, microfilm, or any other means – nor transmitted or translated into a machine language without written permission from the publishers. Registered names, trademarks, etc. used in this book, even when not specifically marked as such, are not to be considered unprotected by law.

Typesetting Uwe Krieg, Berlin

Printing betz-druck GmbH, Darmstadt

Binding Litges & Dopf GmbH, Heppenheim

Wiley Bicentennial Logo Richard J. Pacifico

Printed in the Federal Republic of Germany
Printed on acid-free paper

ISBN: 978-3-527-40602-9

Contents

Preface *XI*

| | | |
|----------|---|----------|
| 1 | Aspects of Nuclear Physics and Astrophysics | 1 |
| 1.1 | History | 1 |
| 1.2 | Nomenclature | 3 |
| 1.3 | Solar System Abundances | 4 |
| 1.4 | Astrophysical Aspects | 8 |
| 1.4.1 | General Considerations | 8 |
| 1.4.2 | Hertzsprung–Russell Diagram | 10 |
| 1.4.3 | Stellar Evolution of Single Stars | 11 |
| 1.4.4 | Binary Stars | 28 |
| 1.5 | Masses, Binding Energies, Nuclear Reactions, and Related Topics | 33 |
| 1.5.1 | Nuclear Mass and Binding Energy | 33 |
| 1.5.2 | Energetics of Nuclear Reactions | 34 |
| 1.5.3 | Atomic Mass and Mass Excess | 37 |
| 1.5.4 | Number Abundance, Mass Fraction, and Mole Fraction | 39 |
| 1.5.5 | Decay Constant, Mean Lifetime, and Half-Life | 42 |
| 1.6 | Nuclear Shell Model | 43 |
| 1.6.1 | Closed Shells and Magic Numbers | 44 |
| 1.6.2 | Nuclear Structure and Nucleon Configuration | 46 |
| 1.7 | Nuclear Excited States and Electromagnetic Transitions | 49 |
| 1.7.1 | Energy, Angular Momentum, and Parity | 49 |
| 1.7.2 | Transition Probabilities | 51 |
| 1.7.3 | Branching Ratio and Mixing Ratio | 53 |
| 1.7.4 | Gamma-Ray Transitions in a Stellar Plasma | 55 |
| 1.7.5 | Isomeric States and the Case of ^{26}Al | 56 |
| 1.8 | Weak Interaction | 58 |
| 1.8.1 | Weak Interaction Processes | 60 |
| 1.8.2 | Energetics | 61 |

| | | |
|----------|---|------------|
| 1.8.3 | Beta-Decay Probabilities | 63 |
| 1.8.4 | Beta-Decays in a Stellar Plasma | 69 |
| 2 | Nuclear Reactions | 75 |
| 2.1 | Cross Sections | 75 |
| 2.2 | Reciprocity Theorem | 77 |
| 2.3 | Elastic Scattering and Method of Partial Waves | 79 |
| 2.3.1 | General Aspects | 79 |
| 2.3.2 | Relationship Between Differential Cross Section and Scattering Amplitude | 81 |
| 2.3.3 | The Free Particle | 82 |
| 2.3.4 | Turning the Potential On | 83 |
| 2.3.5 | Scattering Amplitude and Elastic Scattering Cross Section | 84 |
| 2.3.6 | Reaction Cross Section | 86 |
| 2.4 | Scattering by Simple Potentials | 89 |
| 2.4.1 | Square-Well Potential | 89 |
| 2.4.2 | Square-Barrier Potential | 95 |
| 2.4.3 | Transmission Through the Coulomb Barrier | 103 |
| 2.5 | Theory of Resonances | 108 |
| 2.5.1 | General Aspects | 108 |
| 2.5.2 | Logarithmic Derivative, Phase Shift, and Cross Section | 109 |
| 2.5.3 | Breit–Wigner Formulas | 113 |
| 2.5.4 | Extension to Charged Particles and Arbitrary Values of Orbital Angular Momentum | 117 |
| 2.5.5 | R-Matrix Theory | 122 |
| 2.5.6 | Experimental Tests of the One-Level Breit–Wigner Formula | 126 |
| 2.5.7 | Partial and Reduced Widths | 130 |
| 2.6 | Continuum Theory | 139 |
| 2.7 | Hauser–Feshbach Theory | 141 |
| 3 | Thermonuclear Reactions | 147 |
| 3.1 | Cross Sections and Reaction Rates | 147 |
| 3.1.1 | Particle-Induced Reactions | 147 |
| 3.1.2 | Photon-Induced Reactions | 151 |
| 3.1.3 | Abundance Evolution | 152 |
| 3.1.4 | Forward and Reverse Reactions | 155 |
| 3.1.5 | Reaction Rates at Elevated Temperatures | 159 |
| 3.1.6 | Reaction Rate Equilibria | 164 |
| 3.1.7 | Nuclear Energy Generation | 170 |
| 3.2 | Nonresonant and Resonant Thermonuclear Reaction Rates | 171 |
| 3.2.1 | Nonresonant Reaction Rates for Charged-Particle-Induced Reactions | 171 |

| | | |
|----------|--|------------|
| 3.2.2 | Nonresonant Reaction Rates for Neutron-Induced Reactions | 185 |
| 3.2.3 | Nonresonant Reaction Rates for Photon-Induced Reactions | 189 |
| 3.2.4 | Narrow-Resonance Reaction Rates | 191 |
| 3.2.5 | Broad-Resonance Reaction Rates | 201 |
| 3.2.6 | Electron Screening | 207 |
| 3.2.7 | Total Reaction Rates | 212 |
| 4 | Nuclear Physics Experiments | 219 |
| 4.1 | General Aspects | 219 |
| 4.1.1 | Charged-Particle Beams | 220 |
| 4.1.2 | Neutron Beams | 222 |
| 4.2 | Interaction of Radiation with Matter | 225 |
| 4.2.1 | Interactions of Heavy Charged Particles | 225 |
| 4.2.2 | Interactions of Photons | 236 |
| 4.2.3 | Interactions of Neutrons | 244 |
| 4.3 | Targets and Related Equipment | 247 |
| 4.3.1 | Backings | 249 |
| 4.3.2 | Target Preparation | 250 |
| 4.3.3 | Contaminants | 255 |
| 4.3.4 | Target Chamber and Holder | 256 |
| 4.4 | Radiation Detectors | 258 |
| 4.4.1 | General Aspects | 258 |
| 4.4.2 | Semiconductor Detectors | 263 |
| 4.4.3 | Scintillation Detectors | 267 |
| 4.4.4 | Proportional Counters | 272 |
| 4.4.5 | Microchannel Plate Detectors | 273 |
| 4.5 | Nuclear Spectroscopy | 274 |
| 4.5.1 | Charged-Particle Spectroscopy | 275 |
| 4.5.2 | Gamma-Ray Spectroscopy | 280 |
| 4.5.3 | Neutron Spectroscopy | 299 |
| 4.6 | Miscellaneous Experimental Techniques | 305 |
| 4.6.1 | Radioactive Ion Beams | 306 |
| 4.6.2 | Activation Method | 311 |
| 4.6.3 | Time-of-Flight Technique | 315 |
| 4.7 | Background Radiation | 317 |
| 4.7.1 | General Aspects | 318 |
| 4.7.2 | Background in Charged-Particle Detector Spectra | 321 |
| 4.7.3 | Background in γ -Ray Detector Spectra | 323 |
| 4.7.4 | Background in Neutron Detector Spectra | 331 |
| 4.8 | Yields and Cross Sections for Charged-Particle-Induced Reactions | 334 |
| 4.8.1 | Nonresonant and Resonant Yields | 335 |

| | | |
|----------|---|------------|
| 4.8.2 | General Treatment of Yield Curves | 342 |
| 4.8.3 | Measured Yield Curves and Excitation Functions | 348 |
| 4.8.4 | Determination of Absolute Resonance Strengths and Cross Sections | 352 |
| 4.9 | Transmissions, Yields, and Cross Sections for Neutron-Induced Reactions | 361 |
| 4.9.1 | Resonance Transmission | 362 |
| 4.9.2 | Resonant and Nonresonant Yields | 364 |
| 4.9.3 | Effective Cross Section | 365 |
| 4.9.4 | Measured Yields and Transmissions | 366 |
| 4.9.5 | Relative and Absolute Cross Sections | 368 |
| 5 | Nuclear Burning Stages and Processes | 375 |
| 5.1 | Hydrostatic Hydrogen Burning | 378 |
| 5.1.1 | pp Chains | 379 |
| 5.1.2 | CNO Cycles | 396 |
| 5.1.3 | Hydrostatic Hydrogen Burning Beyond the CNO Mass Region | 410 |
| 5.2 | Explosive Hydrogen Burning | 417 |
| 5.2.1 | Hot CNO Cycles | 418 |
| 5.2.2 | Explosive Hydrogen Burning Beyond the CNO Mass Region | 431 |
| 5.3 | Hydrostatic Helium Burning | 437 |
| 5.3.1 | Helium-Burning Reactions | 439 |
| 5.3.2 | Nucleosynthesis During Hydrostatic He Burning | 446 |
| 5.3.3 | Other Helium-Burning Reactions | 448 |
| 5.4 | Explosive Hydrogen-Helium Burning | 449 |
| 5.4.1 | Breakout from the HCNO Cycles | 450 |
| 5.4.2 | Network Calculations at Constant Temperature and Density | 454 |
| 5.4.3 | Nucleosynthesis for Temperature–Density Profiles | 466 |
| 5.5 | Advanced Burning Stages | 472 |
| 5.5.1 | Carbon Burning | 472 |
| 5.5.2 | Neon Burning | 480 |
| 5.5.3 | Oxygen Burning | 484 |
| 5.5.4 | Silicon Burning | 494 |
| 5.5.5 | Nuclear Statistical Equilibrium and Freeze-Out | 507 |
| 5.6 | Nucleosynthesis Beyond the Iron Peak | 514 |
| 5.6.1 | The s-Process | 518 |
| 5.6.2 | The r-Process | 536 |
| 5.6.3 | The p-Process | 556 |
| 5.7 | Origin of the Solar System Nuclides | 568 |

Appendix

- A Solutions of the Schrödinger Equation in Three Dimensions 575**
 - A.1 Zero Orbital Angular Momentum and Constant Potential 577
 - A.2 Arbitrary Orbital Angular Momentum and Zero Potential 578
 - A.3 Arbitrary Orbital Angular Momentum and Coulomb Potential 578

- B Quantum Mechanical Selection Rules 581**

- C Kinematics 589**
 - C.1 Relationship of Kinematic Quantities in the Laboratory Coordinate System 589
 - C.2 Transformation Between Laboratory and Center-of-Mass Coordinate System 593

- D Angular Correlations 599**
 - D.1 General Aspects 600
 - D.2 Pure Radiations in a Two-Step Process 604
 - D.3 Mixed Radiations in a Two-Step Process 606
 - D.4 Three-Step Process with Unobserved Intermediate Radiation 611
 - D.5 Experimental Considerations 613
 - D.6 Concluding Remarks 615

- E Constants, Data, Units, and Notation 619**
 - E.1 Physical Constants and Data 619
 - E.2 Mathematical Expressions 620
 - E.3 Prefixes and Units 621
 - E.4 Physical Quantities 623

- Color Plates 631**

- References 643**

- Index 653**

Preface

Nuclear processes generate the energy that makes stars shine. The same nuclear processes in stars are responsible for the synthesis of the elements. When stars eject part of their matter through various means, they enrich the interstellar medium with the nuclear ashes and thereby provide the building blocks for the birth of new stars, of planets, and of life itself. The theory of this building of elements is called nucleosynthesis and it is remarkably successful in describing the nuclear processes in stars that are located so far away from us in space and time. It is equally remarkable how the theory predicts these processes based on the quantum mechanical properties of atomic nuclei. Nucleosynthesis, nuclear energy generation in stars, and other topics at the intersection of nuclear physics and astrophysics make up the science of nuclear astrophysics. Like most fields of physics, it involves both theoretical and experimental activities. The purpose of this book is to explain these concepts with special emphasis on nuclear processes and their interplay in stars.

Work on the manuscript for this book started when I was invited to teach a two-week long graduate-level course on “Nuclear Physics of Stars” at the Universitat Politècnica de Catalunya in Barcelona, Spain, in June 2003. During the preparations for the course it became quite obvious that it would be useful to have an up-to-date textbook available. The encouragement I received from many colleagues and students to write such a book was instrumental for my decision to begin work on a manuscript.

After a decade of teaching at the University of North Carolina at Chapel Hill I learned from my students to take no “well-established” fact for granted. They wanted to see derivations of equations when I attempted to state “the obvious.” They insisted on more fundamental explanations when I just tried to “wave my hands.” The style of the present book is certainly influenced by my teaching experience. Indeed, most equations are derived in the text and special emphasis has been placed on the art work. My main intention is to explain complicated concepts in the simplest and most intuitive manner. In some instances, more elegant formulations of concepts have been presented in the literature. For the manuscript these were considered only if I found

it impossible to come up with a simpler explanation. Colleagues frequently wanted to know “which review paper” I used in the preparation of a specific section. My strategy was to consult review articles only after I wrote a complete first draft of the section. That way I was forced to comprehend the subject myself from the beginning and to come up with a coherent presentation.

The present book is directed toward advanced undergraduate students, graduate students, and researchers in the fields of nuclear physics and astrophysics. Chapter 1 starts with the basic concepts in nuclear physics and stellar evolution. Chapter 2 develops the theory of nuclear reactions starting from basic quantum mechanical ideas. Nuclear processes in a stellar plasma are discussed in Chapter 3. Chapter 4 contains the most important experimental information needed in order to perform measurements in nuclear astrophysics. Chapter 5 provides a discussion of the theory of stellar nucleosynthesis. The appendices contain sections on basic solutions of the Schrödinger equation, angular momentum selection rules, kinematics, and the theory of angular correlations. At the end of the text, physical constants, mathematical symbols and physical quantities are listed as an aid for the reader. As a prerequisite, the student should have taken an undergraduate course in modern physics with elementary coverage of wave functions. An undergraduate course in quantum mechanics or nuclear physics would also be helpful, but is not required.

The present book goes into considerable depth and, consequently, restrictions in time and space made it unavoidable for me to omit a number of important topics. The instructor who is using this book may wish to supplement the material presented here with information on primordial nucleosynthesis (J. Rich, *Fundamentals of Cosmology*, Berlin: Springer, 2001), cosmic-ray spallation reactions (E. Vangioni-Flam, M. Cassé and J. Audouze, *Phys. Rep.*, Vol. 333, p. 365, 2000), nucleochronology (J. J. Cowan, F.-K. Thielemann and J. W. Truran, *Ann. Rev. Astron. Astrophys.*, Vol. 29, p. 447, 1991), neutrino astrophysics (J. N. Bahcall, *Neutrino Astrophysics*, Cambridge: Cambridge University Press, 1989), ν -process (Woosley et al., *Astrophys. J.*, Vol. 356, p. 272, 1990), presolar grains (M. Lugaro, *Stardust from Meteorites*, Singapore: World Scientific, 2005) and indirect measurements of astrophysically important nuclear reactions. It is utterly impossible to recommend one, or even a few, references for the last topic which represents a vast field in its own right.

I would certainly not have written this book without the influence of two of my colleagues. I am indebted to Jordi José, who invited me to Barcelona in 2003 and who organized my lectures and my wonderful stay there. I also wish to express my appreciation to Art Champagne, who supported me professionally through all stages during the preparation of the manuscript. A number of people have read through parts of the manuscript and have pro-

vided many valuable suggestions and comments. The book benefited substantially from their input. It is my pleasure to thank Carmen Angulo, Dick Azuma, Bruce Carney, Gerald Cecil, Art Champagne, Alan Chen, Alessandro Chieffi, Alain Coc, Pierre Descouvemont, Ryan Fitzgerald, Uwe Greife, Raph Hix, Jordi José, Franz Käppeler, Karl-Ludwig Kratz, Alison Laird, John Latanzio, Marco Limongi, Richard Longland, Alex Murphy, Joe Newton, Anuj Parikh, Helmut Paul, Tommy Rauscher, Paddy Regan, Hendrik Schatz, Sumner Starrfield, and Claudio Ugalde. I should like to thank Daniel Aarhus for typing the manuscript, and John Kelley for helping with the preparation of some figures. I would like to acknowledge support from a University Research Council publication grant from the University of North Carolina at Chapel Hill and I am also grateful for the support I received from the Triangle Universities Nuclear Laboratory. The book is dedicated to my daughter Alina, my son Kimon, and my wife Andrea, who certainly felt the significant investment of my private time in this project during the past four years.

Carrboro, September 2006

Christian Iliadis

1

Aspects of Nuclear Physics and Astrophysics

1.1 History

In 1920 Aston discovered that the mass of the helium atom is slightly less than four times the mass of the hydrogen atom. Immediately afterward, Eddington suggested in his 1920 presidential address to the British Association for the Advancement of Science that Aston's discovery would explain the energy generation of the Sun via the conversion of hydrogen to helium. However, Eddington could not explain the fact that the stellar temperatures inferred from observation were well below those thought necessary to initiate fusion reactions. In 1928 Gamow, and independently Condon and Gourney, calculated the quantum mechanical probability for particles to tunnel through potential barriers and thereby explained the phenomenon of α -particle decay (Gamow 1928, Condon and Gourney 1929). Atkinson and Houtermans used Gamow's results to suggest that quantum mechanical tunneling may explain the energy generation of stars via fusion reactions (Atkinson and Houtermans 1929).

Cockroft and Walton (1932) initiated the first nuclear reaction using artificially accelerated particles by bombarding and disintegrating lithium nuclei with protons accelerated to several hundred keV energy. Incidentally, the disintegration of lithium into two α -particles is one of the reactions of what would later be called the pp chains. Lauritsen and Crane produced in 1934 a 10-min radioactivity following the bombardment of carbon with protons. It was the first measurement of one of the reactions of what would later be called the CNO cycle.

Atkinson (1936) proposed the fusion of two hydrogen nuclei to deuterium as a source of stellar energy generation. A detailed treatment of this reaction was provided by Bethe and Critchfield who showed that the $p + p$ reaction gives indeed an energy generation of the correct order of magnitude for the Sun (Bethe and Critchfield 1938). The energy production in stars via the CNO cycle was independently discovered by von Weizsäcker (1938) and Bethe (1939). The latter work, in particular, investigated for the first time the rate of energy production and the temperature dependence of the CNO cycle.

In the following years some of the pioneering ideas of nuclear astrophysics were established. In two papers, Hoyle first presented the theory of nucleosynthesis within the framework of stellar evolution by using the nuclear data available at the time (Hoyle et al. 1946, Hoyle 1954). Nuclear experiments had firmly established that no stable nucleus of mass number 5 or 8 exists in nature. For this reason, it was a mystery how these mass gaps could be bypassed in the synthesis of heavier nuclei from lighter species. Salpeter suggested in 1951 that a small equilibrium concentration of unstable ^8Be could capture another α -particle to form stable ^{12}C and that this “triple- α reaction” could be the main energy source in red giant stars (Salpeter 1952). Hoyle pointed out that the capture probability would be far too small unless an excited state with zero spin and positive parity existed in ^{12}C at about 7.7 MeV excitation energy. His remarkable theoretical insight was verified when the level was clearly identified (Dunbar et al. 1953) and its properties determined (Cook et al. 1957), thereby establishing the triple- α reaction as the mechanism to overcome the mass 5 and 8 gaps.

In an influential review, Suess and Urey demonstrated the existence of several double peaks in a greatly improved distribution of observed solar-system abundances (Suess and Urey 1956). It became immediately clear that these abundance peaks were associated with the neutron shell fillings at the magic neutron numbers in the nuclear shell model that Jensen and Goeppert Mayer had developed in 1949. The nucleosynthesis processes for the heavy nuclides beyond iron via neutron captures became later known as the s- and r-process.

Of great importance was the discovery of spectral lines from the element technetium in evolved red giant stars (Merrill 1952). All of the technetium isotopes are unstable and the longest lived isotope has a half-life of $\approx 4.2 \times 10^6$ y. Such half-lives are very short on a cosmological time scale ($\approx 10^{10}$ y) and, consequently, the discovery showed beyond doubt that the technetium must have been produced “recently” within the stars and that the products of nucleosynthesis could indeed reach the stellar surface with the help of mass loss and mixing.

The available knowledge at the time regarding the synthesis of elements was presented in a review article by Burbidge et al. (1957), and independently by Cameron (1957). These papers laid the ground work for the modern theory of nuclear astrophysics. The field has developed since into an exciting discipline with impressive achievements, linking the topics of astronomical observation, nuclear physics experiment, nuclear theory, stellar evolution, and hydrodynamics.

1.2

Nomenclature

Atomic nuclei consist of protons and neutrons. The symbol Z denotes the number of protons and is called *atomic number*. The number of neutrons is denoted by the symbol N . The *mass number* A is defined by the integer quantity $A = Z + N$. It is sometimes also referred to as *nucleon number*. Nuclei with the same number of protons and number of neutrons have the same nuclear properties. They can be represented by the symbol A_ZX_N , where X is the element symbol. Any individual nuclear species is called a *nuclide*. Nuclides with the same number of protons, but different number of neutrons (and hence a different mass number A) are called *isotopes*. Nuclides of the same mass number, but with different numbers of protons and neutrons are called *isobars*. Nuclides with the same number of neutrons, but with different number of protons (and hence a different mass number A) are called *isotones*. Isotopes, isobars, and isotones have different numbers of protons or neutrons and, therefore, their nuclear physics properties are different.

Nuclides can be represented in a two-dimensional diagram, called *chart of the nuclides*. It displays the number of neutrons and protons on the horizontal and vertical axes, respectively. Each square in this diagram represents a different nuclide with unique nuclear physics properties. Figure 1.1 displays a section of the chart of the nuclides, showing the lightest species with $Z \leq 15$ and $N \leq 20$. The shaded squares represent stable nuclides, while the open squares correspond to unstable nuclides with half-lives in excess of 1 ms. It is obvious that many more unstable than stable nuclides exist in nature. It is also striking that no stable nuclides exist with a mass number of $A = 5$ or 8. This circumstance has a profound influence on the nucleosynthesis in stars, as will be seen in Chapter 5.

Example 1.1

The nuclide of carbon ($Z = 6$) with 7 neutrons ($N = 7$) has a mass number of $A = Z + N = 13$ and is represented by the symbol ${}^{13}_6\text{C}_7$. Since the element symbol and the number of protons (atomic number) carry the same information, both $Z = 6$ and $N = A - Z = 7$ are frequently suppressed in the notation. The carbon species with mass number $A = 13$ is then unambiguously described by the symbol ${}^{13}\text{C}$.

The species ${}^{12}_6\text{C}_6$, ${}^{13}_6\text{C}_7$, and ${}^{14}_6\text{C}_8$ are isotopes of carbon ($Z = 6$); ${}^{20}_{10}\text{Ne}_{10}$, ${}^{20}_{11}\text{Na}_9$, and ${}^{20}_{12}\text{Mg}_8$ are isobars of $A = 20$; ${}^{28}_{14}\text{Si}_{14}$, ${}^{29}_{15}\text{P}_{14}$, and ${}^{30}_{16}\text{S}_{14}$ are isotones of $N = 14$.

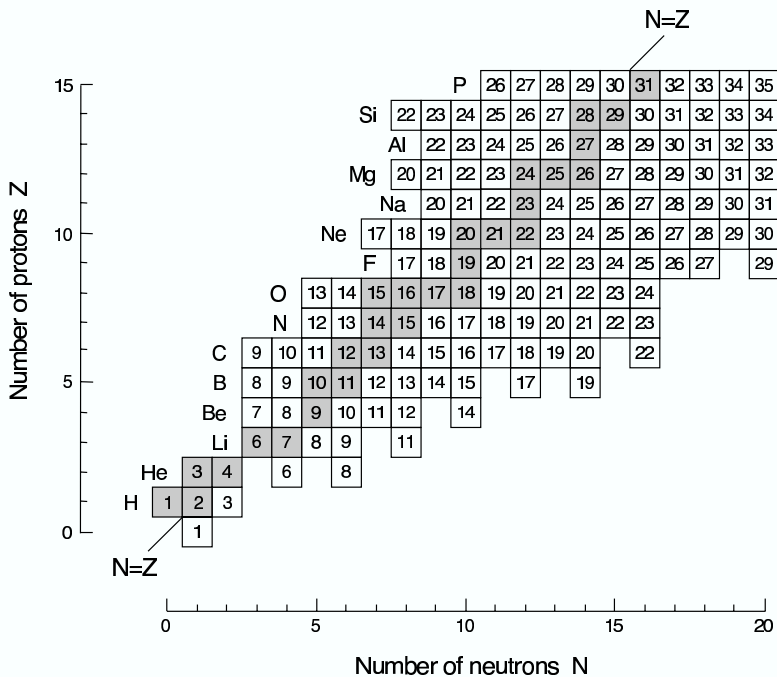


Fig. 1.1 Section of the chart of the nuclides, showing the lightest species with $Z \leq 15$ and $N \leq 20$. The shaded squares represent stable nuclides, while the open squares correspond to unstable nuclides with half-lives in excess of 1 ms. The only exceptions are the nuclides ${}^8\text{Be}$ and ${}^9\text{B}$ which have much shorter half-lives. Note that no stable nuclides exist with a mass number of $A = 5$ or 8.

1.3

Solar System Abundances

It is commonly accepted that the solar system formed from the collapse of a gaseous nebula that had an almost uniform chemical and isotopic abundance distribution. Abundances in the solar system are also similar to those found in many stars, in the interstellar medium of the Sun's neighborhood and in parts of other galaxies. Therefore, it was hoped for a long time that a careful study of solar system abundances would provide a "cosmic" or "universal" abundance distribution, that is, an average abundance distribution which is representative for all luminous matter in the universe. A closer comparison of abundances in the solar system and other parts of the universe shows, however, significant compositional differences. Furthermore, the discovery of presolar grains in primitive meteorites allowed for the first time a very precise chemical and isotopic analysis of interstellar matter. Measurements of isotopic abundances in these presolar grains revealed the existence of very large deviations compared to solar system values. Following common practice in the

recent literature, we will avoid the term “universal” abundances and use instead the expression *solar system abundances* when referring to the abundance distribution in the solar system at the time of its formation. The latter distribution provides an important standard to which reference is frequently made.

There are two major, independent and sometimes complementary, sources of solar system elemental abundances: (i) observations of the solar photosphere, and (ii) analysis of a specific class of meteorites, called *CI carbonaceous chondrites*. The Sun contains most of the mass in the solar system and is, therefore, representative for the overall composition. On the other hand, planets contain much less mass but they underwent extensive chemical fractionation over the past 4.5 Gy since their formation (Cowley 1995). Among the more than 20,000 recovered meteorites, there are only five known CI carbonaceous chondrites. Although they contain a minuscule amount of matter, they are believed to be among the most primitive objects in the solar system. They show the least evidence for chemical fractionation and remelting after condensation and thus they retained most of the elements (except for a few very volatile species) present in the original matter of the solar nebula. Details on how these abundances are obtained will not be repeated here (see, for example, Arnett 1996, Grevesse and Sauval 1998, Palme and Jones 2003, Lodders 2003). It is sufficient to remark at this point that the abundances derived from the solar photosphere and from primitive meteorites are in remarkable overall agreement (better than $\pm 10\%$ for most elements). Solar system *isotopic* abundances are then derived from the *elemental* abundances by using mainly terrestrial isotopic ratios (Rosman and Taylor 1998).

The solar system abundances of the nuclides are shown in Fig. 1.2a versus mass number A . The abundances are normalized to the number of silicon atoms. In cases where two or more stable isobars exist for a specific mass number A , the sum of the individual abundances is shown in the figure. Part b displays the abundances separately for even- A and odd- A nuclides. Almost all the mass is contained in ^1H (71.1%) and ^4He (27.4%). There is an abundance minimum in the $A = 5\text{--}11$ region, corresponding to the elements Li, Be, and B. More than half of the remaining mass (1.5%) is in the form of ^{12}C and ^{16}O . The abundances drop slowly with increasing mass number. Another minimum occurs in the $A = 41\text{--}49$ region, around the element Sc. The abundance curve exhibits a maximum in the $A = 50\text{--}65$ region, near the element Fe. The nuclides in this region are referred to as the *iron peak*. Beyond the iron peak, the abundances in general decrease with increasing mass number, although pronounced maxima are clearly visible in the $A = 110\text{--}150$ and $A = 180\text{--}210$ regions. Closer inspection of Fig. 1.2b also reveals that even- A nuclides are generally more abundant than odd- A nuclides. Furthermore, the abundance curve for odd- A nuclides is considerably smoother than the one for even- A nuclides.

The outstanding gross features in Fig. 1.2 are the abundance maxima and minima. Specifically, the abundances do not scatter randomly, but instead exhibit a certain regularity and systematics. It is reasonable to assume that the abundances within any group or subgroup of nuclides can be attributed primarily to a specific mechanism of nucleosynthesis. Starting with the work of Suess and Urey (1956), such tables of solar system abundances had an enormous influence on investigations of the origin of the elements and the development of nuclear astrophysics. Not only did it become possible to identify and study various processes of nucleosynthesis that left their distinctive signatures in the abundance distribution, but a connection could also be made to the environments in which these sources of nucleosynthesis operated. All nuclides, with few exceptions, are synthesized in stars. Therefore, the observed solar system abundances offer powerful clues to stellar history and evolution, and by extension, to the chemical evolution of the Galaxy as a whole.

It is fascinating that the structures seen in Fig. 1.2 reflect the nuclear physics properties of various processes occurring in nature. A few very general comments follow below. All of the hydrogen (^1H and ^2H) and most of the helium (^3He and ^4He) nuclei originated in the Big Bang (Rich 2001). The most abundant of these, ^1H and ^4He , are the basic building blocks for the synthesis of heavier and more complex nuclei. A deep abundance minimum occurs in the Li–Be–B region. These nuclides are easily destroyed in fusion reactions with protons (that is, their cross sections are very large). Therefore, their observed solar system abundances must be explained by processes that occur in sites other than stellar interiors. They are thought to be produced via spallation reactions induced by Galactic cosmic rays (Vangioni-Flam, Cassé and Audouze 2000). However, the Big Bang and certain stars did most likely contribute to the production of ^7Li . All of the heavier nuclides with $A \geq 12$ are produced in stars. The nuclides in the region between ^{12}C and ^{40}Ca are synthesized via charged-particle nuclear reactions in various stellar burning processes. Reactions between charged particles are subject to the Coulomb repulsion. The larger the charge of the reacting nuclei, the smaller the nuclear reaction probability will become. This circumstance is reflected in the overall decline of the abundance curve from ^{12}C to ^{40}Ca . The abundance maximum of the iron peak is explained by the fact that these nuclides represent energetically the most stable species (Section 1.5.1). Because of the large Coulomb repulsion, the synthesis of nuclides beyond the iron peak via charged-particle reactions becomes very unlikely. These nuclei are instead produced by the capture of neutrons. The abundances of nuclides in the $A > 80$ region are on average a factor of 10^{10} smaller compared to the hydrogen abundance, as can be seen from Fig. 1.2. The observed narrow and broad peaks in this mass region provide unambiguous evidence for the existence of two distinctive neutron capture processes. All of the above comments are very general and do not explain

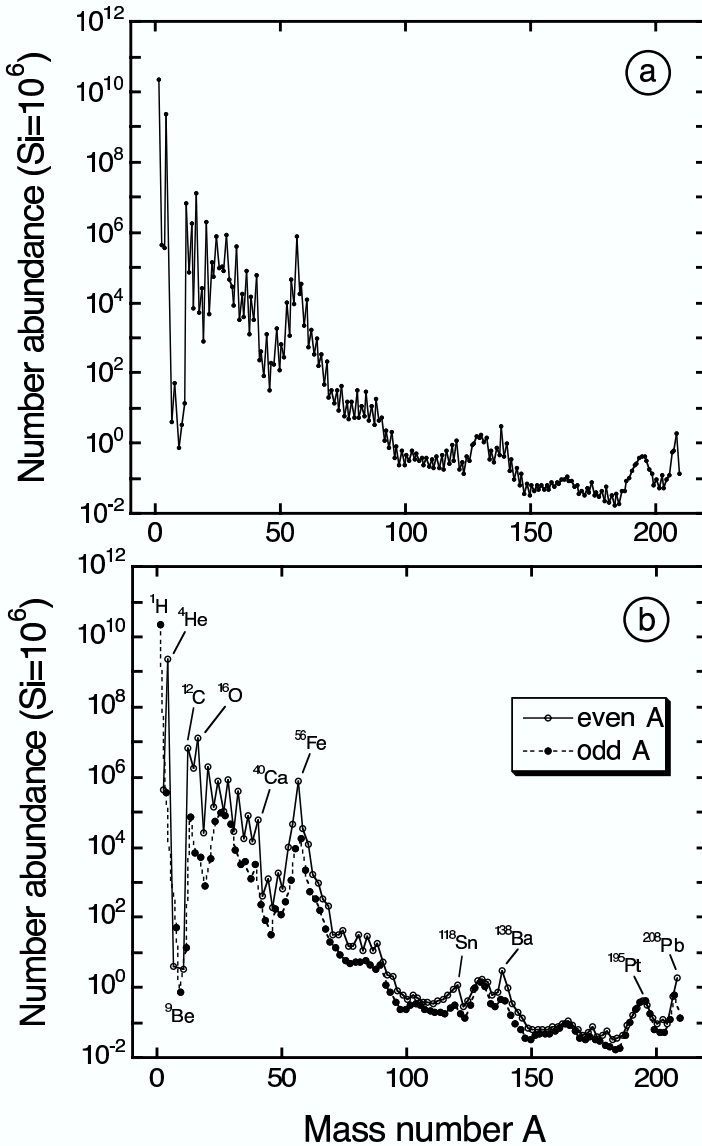


Fig. 1.2 Abundances of the nuclides in the solar system at its birth. Number abundances are normalized to the number of silicon atoms ($\text{Si} = 10^6$). Data from Lodders (2003). (a) Sum of all nuclidic abundances at a given value of A versus mass number.

The maximum in the $A = 50-65$ region is referred to as the iron peak. (b) Separate abundance contributions from nuclides with an even or an odd value of A versus mass number. Even- A nuclides are in general more abundant than odd- A nuclides.

any details of the solar system abundance curve. An extensive discussion of the various nucleosynthetic processes will be given in Chapter 5. Information regarding the origin of the solar system nuclides is provided at the end of this book (Section 5.7).

1.4

Astrophysical Aspects

1.4.1

General Considerations

The study of stars is central to astronomy and astrophysics since stars are long-lived objects that are responsible for most of the visible light we observe from normal galaxies. The fusion of light nuclides into heavier species liberates kinetic energy at the expense of mass and serves as the interior source of the energy radiated from the surface. These very same reactions alter the composition of the stellar matter. As already pointed out, all nuclides with masses of $A \geq 12$ are produced in stars. When a star ejects part of its mass into space during certain evolutionary stages, the chemical composition of the interstellar medium will be altered by the thermonuclear debris. The interstellar medium, in turn, plays a key role in providing material out of which new generations of stars form. This cycling of matter between stars and the interstellar medium involves countless stars. By comparing the age of the Galaxy (≈ 14 Gy) with the age of the Sun (≈ 4.5 Gy) we can conclude that the cycling process that gave rise to the solar system abundance distribution operated for almost 10 billion years.

There is unambiguous *direct* evidence for the nucleosynthesis in stars. First, we already mentioned in Section 1.1 the observation of radioactive technetium in stellar spectra (Merrill 1952). Second, γ -rays from radioactive ^{26}Al were discovered in the interstellar medium by spectrometers onboard satellites (Mahoney et al. 1982, Diehl et al. 1993). The half-life of this nuclide ($\approx 7.17 \times 10^5$ y) is even shorter than that for radioactive technetium, thus demonstrating again that nucleosynthesis is currently active in the Galaxy. Third, neutrinos are predicted to be the byproducts of nuclear processes in stars (Chapter 5). Since they interact very weakly with matter, they escape essentially unimpeded from stellar interiors. Neutrinos from the Sun (Bahcall 1989, Hirata et al. 1990) and from the type II supernova 1987A (Hirata et al. 1987, Bionta et al. 1987) were detected on the Earth, providing another direct test of stellar nucleosynthesis. Fourth, models of supernovae predict the ejection of radioactive ^{56}Ni (half-life of 6 days), which then decays to the radioactive daughter nucleus ^{56}Co (half-life of 77 days). The subsequent decay of this nuclide (to stable ^{56}Fe) is predicted to determine the decline of the light emission from these

stellar explosions. The predictions agree well with the observed light curves of supernovae. Furthermore, photons from the radioactive decay of ^{56}Co have been detected directly from supernova 1987A (Matz et al. 1988, Tueller et al. 1990).

The discovery of the existence of two distinct stellar populations by astronomers was also of paramount importance in this respect. The populations are referred to as population I and population II stars. They differ in their age and their content of metals, by which astronomers mean any element other than hydrogen and helium. Population I stars include the Sun and are metal rich. They are young stars, having formed within the past few billion years, and can be found in the disk of the Galaxy. Extreme population I stars represent the youngest, most metal-rich stars and are found in the spiral arms of the Galaxy. Population II stars, on the other hand, are metal poor. They are relatively old and are found in the halo and the bulge of the Galaxy. Extreme population II stars represent the oldest, most metal poor stars and are found in the halo and in globular clusters. Their metal abundance, relative to hydrogen, is smaller by a factor of 100 or more compared to population I stars.

If one assumes that the initial composition of the Galaxy was uniform and if there exists no mechanism capable of concentrating the metals in the disk of the Galaxy, then the Galaxy must have synthesized an overwhelming fraction of its own metals. This argument provides strong support for the theory that nucleosynthesis is a natural process to occur during the evolution of stars. It is then obvious that the metal content of the Galaxy increases with time since the matter out of which stars form is being cycled through an increasing number of stellar generations. Therefore, the differences in metallicity between the two stellar populations suggest that population I stars formed later during the history of the Galaxy when the interstellar medium became much more metal rich.

Nuclear reactions not only explain the bulk solar-system abundance distribution, but are also indispensable for explaining the observed chemical composition of individual stars. Such observations, even for trace elements, are crucial for constraining theoretical models of stars and for better understanding the complicated interplay of stellar hydrodynamics, convection, mixing, mass loss, and rotation. Stellar nucleosynthesis also plays a decisive role for explaining the chemical composition of the interstellar medium and is thus intertwined with γ -ray astronomy, the study of primitive meteorites, and the nature of cosmic rays.

1.4.2

Hertzsprung–Russell Diagram

The total amount of radiation emitted per unit time, or the *luminosity*, varies strongly from star to star. The same holds for the effective stellar surface temperature. However, if we plot these two quantities for many individual stars in a diagram, then the result is not a random scatter of points, but most stars fall into several distinct groups. This correlation of stellar luminosity and effective surface temperature represents the single most important relationship of stellar properties. It is referred to as *Hertzsprung–Russell diagram* or *color-magnitude diagram*. The latter name results from the fact that surface temperature can be expressed in terms of the color of the star, while luminosity is related to the absolute magnitude. An explanation of these relationships can be found in any introductory astronomy textbook. The Hertzsprung–Russell diagram has a profound influence on the theory of stellar evolution and, by extension, on the history of the Galaxy as a whole.

Consider first Fig. 1.3a, showing a Hertzsprung–Russell diagram for a sample of ≈ 5000 stars in the solar neighborhood. Each dot corresponds to a single star. The surface temperature increases from right to left in the figure. The vast majority of stars occupy the *main sequence* (MS), stretching diagonally from the upper left (hot and bright stars) to the lower right (cool and faint stars). The Sun, for example, belongs to the main sequence. In the low and right part (cool and faint stars) of the main sequence one finds the *red dwarfs* (RD). The *subgiant branch* (SGB) joins the main sequence and extends in a direction to cooler and brighter stars, where the populated region turns first into the *red clump* (RC), and then into the *red giant branch* (RGB). In a region corresponding to smaller luminosity and higher temperature (lower left), one finds a group of faint and hot stars known as *white dwarfs* (WD). A well-known example is Sirius B, the companion of Sirius. Some stars are located below the main sequence, but are much brighter than white dwarfs. These are known as *subdwarfs* (SD). A number of star categories do not appear in the figure. *Supergiants* (SG) are the brightest stars in the Galaxy and would occupy the upper end of the Hertzsprung–Russell diagram, but are very rare in the solar neighborhood. The cool and faint *brown dwarfs* would appear off scale way down in the lower-right part of the figure, but are too faint to appear in the figure.

A Hertzsprung–Russell diagram for the globular cluster M 3 is shown in Fig. 1.3b. There are about 200 globular clusters in the Galaxy. They are located in a spherical space surrounding the Galactic center, called the halo of the Galaxy. Each cluster consists of 10^4 – 10^6 gravitationally bound stars, which are highly concentrated toward the cluster center. An image of the globular cluster M 10 is shown in color Fig. 1 on page 631. Spectroscopic observations revealed that globular clusters are metal poor compared to the Sun, implying that they are rather old and that they formed during the early stages of Galac-

tic evolution. It is commonly accepted that all stars in a typical globular cluster formed around the same time from material of very similar composition. The observation that the stars of a globular cluster occupy distinct regions in the Hertzsprung–Russell diagram must then be explained by differences in the only other major stellar property, that is, their initial mass. As will be shown below, the stellar mass is the most important property influencing the evolution of stars. In fact, the higher the mass, the faster a star will evolve.

Figure 1.3b shows some of the same stellar categories already mentioned in connection with part (a). The densest region is occupied by main-sequence stars. The distinctive kink extending from the main sequence toward cooler and brighter stars is called the *turn-off point* (TO). The subgiant branch stars (SGB) are located on a horizontal part stretching toward the right, which turns upward into the red giant branch (RGB). Three more groups of stars can be clearly distinguished on the left-hand side of the RGB: the asymptotic giant branch (AGB), the red horizontal branch (RHB), and the blue horizontal branch (BHB). As will be seen below, the different groups of stars seen in parts (a) and (b) correspond to different stages of stellar evolution. Globular clusters in particular play an outstanding role in astrophysics since the distinct features in their Hertzsprung–Russell diagrams represent strong constraints for stellar models.

1.4.3

Stellar Evolution of Single Stars

One of the most important goals of the theory of stellar structure and evolution is to understand why certain stars appear only in specific regions of the Hertzsprung–Russell diagram and how they evolve from one region to another. Our aim in this section is to summarize without detailed justification the most important issues related to the nuclear physics of stars. An introduction to stellar evolution can be found in Binney and Merrifield (1998) or Iben (1985). A more comprehensive account is given, for example, in Kippenhahn and Weigert (1990). We will use in this section expressions such as hydrogen burning, helium burning, pp chain, CNO cycle, and so on, to obtain a general idea regarding nuclear processes in stars. These will be explained in depth in Chapter 5.

Theoretical models of stars in hydrostatic equilibrium are constructed in the simplest case by solving a set of four partial differential equations (for radius, luminosity, pressure, and temperature) that describe the structure of a star as a function of the distance from the center and as a function of time. A time sequence of such solutions, or stellar models, represents an *evolutionary track* in the Hertzsprung–Russell diagram. Stellar structure and evolution calculations rely heavily on large scale numerical computer codes. The time changes in the stellar properties are closely related to the energy budget. Energy is generated

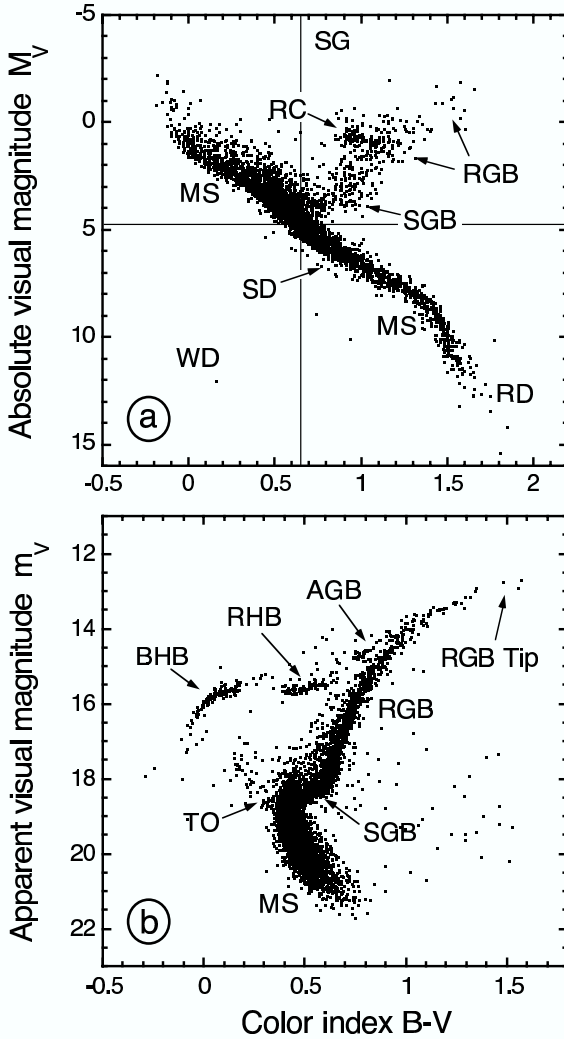


Fig. 1.3 Observational Hertzsprung–Russell diagrams, showing visual magnitude versus color index $B-V$. Each dot corresponds to a star. See the text for an explanation of the labels. (a) Sample of ≈ 5000 stars in the solar neighborhood with precisely known distances. The data were acquired by the Hipparcos astrometry satellite. The vast majority of stars occupy the main sequence, stretching diagonally from the hot (blue) and luminous upper left to the cool (red) and faint lower right. The cross hair indicates the position of the Sun. Cer-

tain categories of stars do not appear in the figure, for example, supergiants (SG), which are rare in the solar neighborhood, and brown dwarfs, which are too faint for detection by Hipparcos. (b) Data for the globular cluster M 3. Apparent rather than absolute magnitude is displayed on the vertical axis since the stars have the same distance from the Earth. The RR Lyrae variable stars, located between the red (RHB) and blue (BHB) horizontal branches, are omitted. From Corwin and Carney (2001).

by the star via nuclear reactions and gravitational contraction, while energy is continuously lost from the stellar surface via emission of photons and neutrinos. As will become clear in the following discussion, a star spends most of its nuclear burning time fusing hydrogen to helium on the main sequence. Careful observations showed that there is a direct correlation between the mass and the luminosity of a main-sequence star. The greater the total mass of the star, the greater the temperature and pressure in the core, the faster nuclear energy is generated, and the greater the energy output or the luminosity of the star. For example, a $10 M_{\odot}$ main-sequence star has ≈ 3000 times the luminosity of the Sun. Furthermore, the main-sequence lifetime will also depend strongly on the stellar mass because a star burns the nuclear fuel at a rate that is determined by its luminosity. For example, solar-metallicity stars with masses of $1 M_{\odot}$, $5 M_{\odot}$, and $15 M_{\odot}$ spend about 10 Gy, 100 My, and 12 My, respectively, on the main sequence. Once a star leaves the main sequence, the evolution speeds up significantly, as will be seen below.

Modern theories have been enormously successful in describing the properties of stars. Nevertheless, many open questions remain unsolved. Stellar evolution is an active research field and it is worthwhile to keep in mind the uncertainties in the model calculations. These reflect our incomplete knowledge of certain processes in stars, including the treatments of energy transport via convection, mass loss, atomic diffusion, turbulent mixing, rotation, and magnetic fields. For binary stars (Section 1.4.4), a host of additional problems is encountered because, first, the model assumption of spherical symmetry must be relaxed and, second, the interaction between the two stars becomes important. We will not discuss these effects in any detail other than to mention that most of them become increasingly important with ongoing stellar evolution. The effects of nuclear physics are deeply intertwined with these issues. When we discuss in later chapters the impact of nuclear physics uncertainties on the nuclear energy generation and the nucleosynthesis, it is very important to keep in mind that we are referring only to one piece in a complex puzzle. One of the main goals in nuclear astrophysics is to better understand the inner workings of stars. To this end, a reliable knowledge of nuclear physics is indispensable.

A chart showing the main evolutionary phases for single stars of various initial masses is shown in Fig. 1.4 and will be helpful for the subsequent discussions. The stellar masses are shown on the left-hand side and time increases from left to right.

Pre-main-sequence stars

When an interstellar gas cloud consisting mainly of hydrogen and helium contracts, gravitational potential energy is transformed into thermal energy and into radiation. The gas is initially in gravitational free fall and most of the lib-

| | | | | | | | | | | | | |
|-------|------------------------|--------------------|---------------------|---------------------|---------------------------|---------------------------|---|---------------------------|---------------------------|--------------|-------|--------|
| 0.013 | Brown dwarf | D-C | | | | | | | | | | |
| 0.08 | Red dwarf | H-C [MS] | | | | | | | He WD | | | |
| 0.4 | Low mass star | H-C [MS] | pp CNO | H-S [RGB] | 1. D U | HeF | He-C | He-S | 3. D U | PNN | CO WD | |
| 1.5 | | | | | | | H-S [HB,RC] | H-S [AGB] | | | | |
| 2 | Intermediate mass star | H-C [MS] | H-S [RGB] | 1. D U | He-C H-S | He-C H-S | He-S H-S [AGB] | | 3. D U | PNN | CO WD | |
| 4 | | H-C [MS] | | | | | 2. He-S D H-S U [AGB] | | | | | |
| 9 | | H-C [MS] | H-S [RGB] | 1. D U | He-C H-S | He-S | 2. He-S D H-S U [AGB] | He-S | 3. D U | PNN | CO WD | |
| 11 | Massive star | H-C [MS] | H-S [RGB] | 1. D U | He-C H-S | C-C He-S | Ne-C C-S | O-C Ne-S | Si-C O-S | 3. D U | PNN | One WD |
| 100 | | | | | | | | | | | | |

Fig. 1.4 Major evolutionary stages for single stars in different mass ranges. The initial stellar mass is given on the left-hand side. Time increases from left to right. The nuclear fuel in each burning phase is shown in bold. For example, “H-C” refers to hydrogen burning in the core, “He-S” denotes helium burning in a shell, and so on. For lower-mass stars, the meaning of the labels in square brackets is described in the text (see also caption of Fig. 1.5); “DU” de-

notes the different dredge-up events. For massive stars, the three dots indicate that there are additional overlying burning shells (Fig. 1.6); the labels are: “CC” for core collapse, “SN” for supernova, “NS” for neutron star, and “BH” for black hole. Note that the mass ranges are approximate estimates only and depend on the stellar metallicity. For the evolution of stars in the mass range of $M \geq 100 M_{\odot}$, see Woosley, Heger and Weaver (2002), and references therein.

erated energy is not retained but radiated away because the gas is relatively transparent. With increasing density, the opacity increases as well and some of the emitted radiation is retained in the cloud. As a result, the temperature and the pressure begin to rise and the contraction of the central, denser part of the cloud slows down. The increasing temperature causes first a dissociation of hydrogen molecules into atoms, and then an ionization of hydrogen and helium atoms. When a temperature of about 10^5 K is reached, the gas is essentially ionized. The electrons trap radiation efficiently and, as a result, the pressure and temperature increase and the collapse of the central part of the cloud halts. The pre-main-sequence star eventually reaches a state of hydrostatic equilibrium, while still accreting matter from the outer parts of the cloud.

The source of energy is gravitational contraction, but the first nuclear reactions start to occur when the central temperature reaches a few million kelvin. Primordial deuterium fuses with hydrogen, a process that is called *deuterium*

burning (Section 5.1.1), and primordial lithium may be destroyed via interactions with protons (${}^7\text{Li} + \text{p} \rightarrow \alpha + \alpha$; the notation will be explained in Section 1.5.2). At this stage, energy is transported via convection and most of the star's matter, including surface material, is expected to be processed through the center. Although the nuclear energy release is very small, the reactions change the light element abundances and thus provide valuable information on the central temperatures.

When the temperature reaches several million kelvin, the fusion of hydrogen to helium starts to occur and contributes an increasing fraction to the total energy output. Ultimately, a point will be reached where hydrogen fusion in the core becomes the only source of energy. The star is now in hydrostatic and thermal equilibrium and has reached a location in the Hertzsprung–Russell diagram that is referred to as the *zero age main sequence* (ZAMS). Stars with different initial masses reach the main sequence at different times. For example, the premain-sequence evolution of a $1 M_{\odot}$ star lasts about 75 million years. Different stellar masses populate different locations on the zero age main sequence, which thus represents a line in the Hertzsprung–Russell diagram. Massive stars have higher temperatures, initiate nuclear reactions earlier, and are therefore located on the hotter and brighter part (upper left), while less massive stars will be found on the cooler and fainter part (lower right).

Newly born stars are difficult to observe because they are usually surrounded by a rotating disk of gas and dust. The solar system, for example, presumably formed from such a disk. An example for premain-sequence objects is the *T Tauri stars*. Their lithium abundance is relatively high, indicating that the central temperature has not yet reached large enough values to destroy lithium via nuclear reactions involving protons.

The subsequent fate of stars depends strongly on their initial mass. We will consider the different mass ranges in turn. These main divisions are not sharp but depend somewhat on the chemical composition.

Initial mass of $0.013 M_{\odot} \lesssim M \lesssim 0.08 M_{\odot}$

Theory predicts that objects in this mass range never reach the central temperatures required to sustain hydrogen fusion in their cores and are thus unable to generate sufficient nuclear energy to provide pressure support. The search for these very faint and cool stars provides important constraints for stellar evolution theory. Such objects have only been discovered in the mid-1990s and are referred to as *brown dwarfs*. They are predicted to be very abundant in the Galaxy and are, therefore, candidates for the elusive (baryonic) dark matter. Brown dwarfs are fully convective and their energy source in the early stages is provided by gravitational contraction.

Although brown dwarfs are not true stars, they do have enough mass to undergo deuterium burning, a fact that sets them apart from massive planets

like Jupiter. This provides an additional, low-level, source of energy. They also have a relatively high lithium abundance since temperatures remain too low to destroy this element. The outer layers of a brown dwarf can be described by the ideal gas law. The core, however, becomes eventually electron degenerate. As a result, the contraction halts and the brown dwarf slowly cools, at approximately constant radius, by radiating its thermal energy into space. In the Hertzsprung–Russell diagram, a brown dwarf evolves almost vertically downward and straight past the main sequence (Fig. 1.3).

A detailed description of the properties of degenerate matter is given in many modern physics textbooks and is not repeated here. We will summarize a few properties, however, that are also important for our discussion of other stars. Matter becomes degenerate at relatively high densities as a result of the Pauli exclusion principle which states that no more than two spin-1/2 particles (such as electrons) can occupy a given quantum state simultaneously. A degenerate gas strongly resists further compression because electrons cannot move into lower energy levels that are already occupied. Unlike an ideal classical gas, whose pressure is proportional to its temperature, the pressure exerted by a completely degenerate gas does not depend on temperature. Or, in other words, increasing the temperature of a partially degenerate gas has only a small effect on the total pressure. It will be seen later that, when the temperature reaches a sufficiently high value, the degeneracy is lifted, by which we mean that the properties of such a gas revert to those of an ideal classical gas. Furthermore, there exists an upper limit to the pressure provided by a degenerate gas. If gravity exceeds this pressure, the star will collapse despite the presence of the degenerate particles. The maximum value for the mass of a star that can maintain an equilibrium between degeneracy pressure and gravity is called the *Chandrasekhar limit*. Its precise value depends on the composition. For an electron degenerate gas and matter characterized by two nucleons per electron (for example, ${}^4\text{He}$, ${}^{12}\text{C}$, or ${}^{16}\text{O}$), the limiting value amounts to $\approx 1.44 M_{\odot}$. Stars that enter a state of electron degeneracy toward the end of their evolution are called *white dwarfs*. Indeed, white dwarfs with masses in excess of the Chandrasekhar limit are not observed in nature.

Initial mass of $0.08 M_{\odot} \lesssim M \lesssim 0.4 M_{\odot}$

Stars in this mass range are sometimes referred to as *red dwarfs* (or M dwarfs). They are the most common type of star in the neighborhood of the Sun. For example, the nearest star to the Sun, Proxima Centauri, is a red dwarf. These stars have sufficient mass to fuse hydrogen to helium (*hydrogen burning*) in their cores via the pp chain. Starting from the zero age main sequence, the red dwarf evolves toward higher luminosity and increasing surface temperature (up and left). All stars that sustain hydrostatic equilibrium by burning hydrogen in their cores are called *main-sequence stars*. Theoretical models indi-

cate that, for example, a $0.1 M_{\odot}$ star of solar metallicity remains on the main sequence for about 6000 Gy. During this time the red dwarf is fully convective, which implies that its entire hydrogen content is available as nuclear fuel. Since the age of the Universe is about 14 Gy, all red dwarfs that we observe must be main-sequence stars. Eventually, they will run out of nuclear fuel, that is, all their hydrogen will be converted to helium. Red dwarfs do not have enough mass to produce the higher temperatures required to fuse helium nuclei. Thus they contract until electron degeneracy sets in. Their volume is constant from then on since the degeneracy pressure resists further compression. They become helium white dwarfs that cool slowly by radiating away their thermal energy.

Initial mass of $0.4 M_{\odot} \lesssim M \lesssim 2 M_{\odot}$

The evolution of stars in this mass range is considerably more complicated compared to the previous cases. The life of the star starts on the zero age main sequence when hydrogen begins to fuse to helium in the core. In stars with masses below $M \approx 1.5 M_{\odot}$, hydrogen fusion proceeds via the pp chains, while more massive stars burn hydrogen via the CNO cycles. It will be seen later that these different processes affect the stellar structure since they possess very different temperature dependences (Section 5.1). In stars with $M \gtrsim 1.5 M_{\odot}$, the strong temperature dependence of the CNO cycles concentrates the energy production in the center and, as a result, the core transports energy via convection. In stars with $M \lesssim 1.5 M_{\odot}$, the energy generated in the core by the pp chains is transported via radiation.

As an example, we will discuss in the following the evolution of a special star, the Sun (see color Fig. 2 on page 632). The evolutionary track is shown schematically in Fig. 1.5a. The arguments given below follow the numerical results obtained by Sackmann, Boothroyd and Kraemer (1993). The Sun started central hydrogen burning via the pp chains on the zero age main sequence about 4.5 Gy ago. At present the central temperature and density amount to $T \approx 15$ MK and $\rho \approx 150$ g/cm³, respectively, and about one half of the original hydrogen in the core has been consumed so far. The Sun has a very small convective region at the surface, comprising only $\approx 2\%$ of its entire mass. About 4.8 Gy from now, the hydrogen in the core will be exhausted. The Sun will then be located at the bluest and hottest point on the main sequence, called the *turn-off point*. Note that in Fig. 1.5a the track describing nuclear burning on the main sequence follows an arc. This is one of the reasons for the fact that the main sequence in observational Hertzsprung–Russell diagrams represents a band rather than a narrow line.

Hydrogen fusion continues in a thick shell near the core where there is still hydrogen left. The Sun slowly leaves the main sequence at this point. The Sun's center begins to contract in order to generate energy that is no longer

provided by nuclear processes and the contraction causes further heating. As a result, the temperature in the hydrogen burning shell, and the associated nuclear energy generation rate, also increase. Initially, the Sun has not yet developed a fully convective envelope and it is called a *subgiant branch star* (SGB). Eventually, the envelope becomes fully convective. The extra energy output from the hydrogen burning shell results in a dramatic surface expansion and engulfs the planet Mercury. The Sun becomes a red giant star. While the Sun ascends the red giant branch (RGB), the luminosity increases continuously. Maximum luminosity is achieved on the tip of the red giant branch after about 0.6 Gy from the time when the Sun left the main sequence. During the red giant phase the Sun starts to experience significant mass loss. The contraction of the core during the red giant phase increases the central temperature and density by factors of 10 and 10^4 , respectively, compared to the values at hydrogen ignition. In fact, the core achieves such high densities that the matter becomes electron degenerate. During the RGB phase, the convective envelope deepens significantly until it comprises about 75% of the Sun's mass. This deep convective envelope dredges up the products of hydrogen burning from the outer core. The process is referred to as the "first dredge-up."

When the temperature reaches about $T \approx 0.1$ GK, the helium in the core starts to fuse to carbon and oxygen (*helium burning*). In a normal gas, the extra energy release would cause an expansion. As a result, the temperature would fall and the nuclear energy generation rate would decrease as well. This is the usual manner by which stars adjust to an energy increase in their interior, allowing them to stabilize. However, in a degenerate gas the temperature increase does not affect the pressure. No expansion occurs and, as a result, the temperature increases causing an even higher energy generation rate. As will be seen in Section 5.3, helium burning is highly temperature sensitive. The sequence of events repeats itself, giving rise to a *thermonuclear runaway*. It only terminates after so much energy has been released that the electron degeneracy is lifted. Thus, the ignition of helium in the core results in a violent *core helium flash* (HeF).

It is important to point out that the helium flash does not represent a stellar explosion. The energy during the thermonuclear runaway goes into lifting the electron degeneracy and into the subsequent expansion of the core. The surface luminosity of the star does not increase. In fact, the opposite happens. The surface luminosity declines by two orders of magnitude because the expansion of the core causes the surrounding hydrogen burning shell, which has been supplying all the surface luminosity, to cool and to generate less energy. Eventually, the Sun becomes a *horizontal branch star*, quietly burning helium in the core. The temperatures in the hydrogen shell just above the core are high enough for hydrogen to continue to burn via the CNO cycles. The nuclear

energy release in helium fusion is considerably less compared to hydrogen fusion. Therefore, the duration of the core helium burning stage is much shorter than that of the core hydrogen burning stage. The Sun remains on the horizontal branch for about 0.1 Gy, which is typical for all stars in this mass range.

When the helium in the core is exhausted, the core contracts again, heats up, and ignites the helium in a surrounding shell. The Sun now burns nuclear fuel in two shells, helium in a shell surrounding the carbon–oxygen core, and hydrogen in a shell surrounding the helium burning region. The two shells are separated by an intershell region consisting mainly of helium. This stage is referred to as the early asymptotic giant branch phase (E-AGB), because the second ascent of the giant branch merges almost asymptotically with the first giant branch (at least for some stellar masses). While the Sun ascends the asymptotic giant branch, the helium burning shell becomes thermally unstable (Schwarzschild and Härm 1965; see also Section 5.6.1). Energy is not generated at a steady rate, but the hydrogen and helium burning shell alternate as the major contributor to the overall luminosity. For about 90% of the time, the hydrogen burning shell provides the Sun’s nuclear energy, while the helium shell is only marginally active. Hydrogen burning adds continuously to the mass of the helium zone, however, so that the temperature and density near this zone rise until energy is generated by helium burning at a rate that is larger than the rate at which it can be carried outward by radiative diffusion. As a result, a thermonuclear runaway occurs. The sudden release of energy pushes out and cools the hydrogen burning shell until it ceases to burn. The helium burning shell is now the only source of nuclear energy. Eventually, the expansion quenches the helium shell flash (or *thermal pulse*) and the Sun contracts again. The hydrogen burning shell reignites and ultimately takes over as the dominant nuclear energy source, until the next thermal pulse occurs about 10^5 y later. The cycle may repeat many times. This evolutionary stage is called the thermally pulsing asymptotic giant branch (TP-AGB). The total amount of time the Sun spends on the AGB amounts only to about 20 My and is thus very short compared to the main-sequence lifetime. The thermal pulses cause the Sun’s radius to vary periodically by a factor of 4, with the peak radius reaching close to the Earth.

The Sun suffers an episode of significant mass loss on the asymptotic giant branch via a strong stellar wind. Thermal pulses are ceasing at this point as the Sun becomes a postasymptotic giant branch star (P-AGB), with only a fraction of its initial mass left and the other part returned to the interstellar medium. As more hydrogen of the envelope is ejected into space, hotter layers are uncovered and the Sun begins to move in the Hertzsprung–Russell diagram toward higher surface temperatures (horizontally to the left). When the surface of the Sun becomes hot enough, the intense ultraviolet radiation ionizes the expanding ejecta, which begin to fluoresce brightly as a *planetary*

nebula (PN). Two examples for planetary nebulae, the Dumbbell Nebula and the Cat's Eye Nebula, are shown in color Figs. 3 and 4 on page 633 and 634, respectively. The residual core is called a *planetary nebula nucleus* (PNN). Eventually, there is no hydrogen envelope left and the hydrogen burning shell extinguishes. The luminosity decreases rapidly causing the evolutionary track to turn downward and slightly to the right. The Sun will then end its existence as a white dwarf with a mass of $\approx 0.5 M_{\odot}$, consisting mainly of carbon and oxygen. It is supported by electron degeneracy pressure and cools slowly by radiating away its thermal energy.

It must be stressed again that in the above discussion the evolution beyond the red giant branch is rather uncertain because of our incomplete knowledge on how to predict convection and mass loss. That these effects will indeed occur has been demonstrated by stellar observations, but a deeper understanding is lacking at present. It is generally accepted that each thermal pulse during the TP-AGB phase provides favorable conditions for another dredge-up episode after the end of flash-burning in the helium shell. The convective envelope reaches deep into the star below the bottom of the hydrogen burning shell and carries the products from hydrogen and helium shell burning, in particular helium and carbon, to the stellar surface. This process is referred to as the "third dredge-up" and increases the carbon abundance in the envelope relative to other elements, for example, oxygen. Stars for which the number ratio of carbon to oxygen exceeds unity are called *carbon stars*. Many of these have been observed and most are believed to correspond to stars in their TP-AGB phase. As will be seen later, AGB stars are also the source of many heavy nuclides with mass numbers beyond $A = 60$. Stellar models predict that these (s-process) nuclei are also dredged up to the surface where they can be observed in stellar atmospheres. In fact, the first direct evidence that nucleosynthesis takes place in stars and that the products could be mixed to the surface was the observation of radioactive technetium in certain (S-type) carbon stars (Section 1.1). For more information on AGB stars, see Habing and Olofsson (2004).

We are now in a position to understand some other details in the observational Hertzsprung–Russell diagrams shown in Fig. 1.3. The precise location in luminosity and surface temperature of a star on the horizontal branch depends on the chemical composition of the envelope, the size of the helium core at the time of the helium flash, and the mass of the envelope which is influenced by the mass loss during the preceding RGB phase. In a globular cluster, all the stars start out with the same, low-metallicity, composition and their location on the horizontal branch is mainly influenced by mass loss. The more the mass lost from the hydrogen envelope, the hotter the layers in the star are uncovered. Stars with the smallest amount of mass in the hydrogen envelope populate the blue part (BHB), while stars with more hydrogen left

in the envelope can be found on the red part (RHB). The horizontal branch intersects the so-called instability strip (which is not related to nuclear burning). Stars located in this narrow and almost vertical band, indicated by the two vertical dashed lines in Fig. 1.5a, are unstable to radial pulsation and are called *RR Lyrae variables*. Their luminosity correlates with both their period (several hours to ≈ 1 day) and their metallicity. Therefore, they are important for determining the distances to globular clusters and for establishing a cosmic distance scale (Binney and Merrifield 1998). Increasing the metallicity has the overall effect of making a star fainter and cooler. Therefore, stars in metal-rich clusters or in the solar neighborhood (Fig. 1.3) accumulate at the red end (right) of the horizontal branch, fairly independent of their envelope mass. This region is called the *red clump* (RC).

The metallicity argument also applies to the subdwarfs (SD). These are in fact main-sequence stars of very low metallicity. They are hotter than solar-metallicity stars at a comparable evolutionary stage and are thus located to the left of the main sequence that is occupied by metal-rich stars.

It should also be clear now why the upper part of the main sequence in Fig. 1.3b is missing. Globular clusters are metal-poor and old, and do not form new stars. The high-mass stars that were originally located on the upper part of the main sequence evolved a long time ago into red giants. Only the slowly evolving low-mass stars are left today on the main sequence. Clearly, with increasing time lower mass stars will eventually become red giants and the main sequence will become shorter. It is interesting that the age of the cluster can be determined from the location of the turn-off point, which is located at the top of the surviving portion of the main sequence. If the distance to the cluster is known by independent means, the luminosity of the stars at the turn-off point can be related to their mass. Stellar evolution models can predict the main-sequence lifetime of stars with a given mass, which must then be nearly equal to the age of the cluster. Such investigations yield ages for the most metal-poor (and presumably oldest) globular clusters of about 12–13 Gy, indicating that these objects formed very early in the history of the Galaxy. This estimate also represents an important lower limit on the age of the Universe (Krauss and Chaboyer 2003).

Initial mass of $2 M_{\odot} \lesssim M \lesssim 11 M_{\odot}$

We can divide this mass range into several subranges. Stars with initial masses of $2 M_{\odot} \lesssim M \lesssim 4 M_{\odot}$ evolve obviously faster than less massive stars and their tracks will look quantitatively different from the results shown in Fig. 1.5a. But otherwise they evolve through the same stages as a solar-like star. A major difference, however, arises from the fact that for stars with $M \gtrsim 2 M_{\odot}$ the helium core during the RGB phase does not become electron degenerate. Therefore, a helium flash does not occur but instead helium

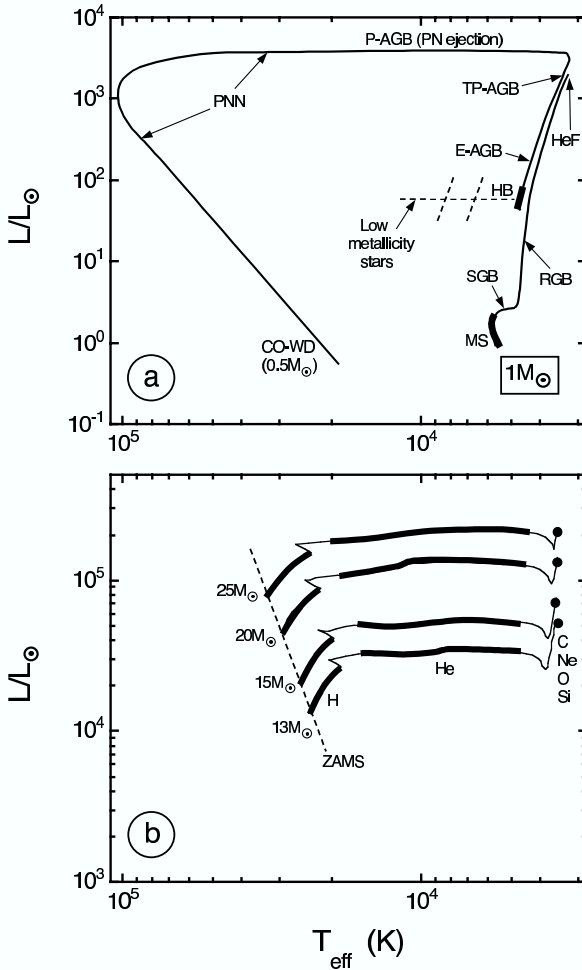


Fig. 1.5 Schematic evolutionary tracks of (a) the Sun, and (b) massive stars of initial solar composition, in the Hertzsprung–Russell diagram; the luminosity on the vertical axis is given in units of the present solar luminosity. The heavy portions define the locations where major core nuclear burning phases occur. Details of tracks during transitions between major nuclear burning phases are omitted. The meaning of the labels are: main sequence (MS); zero age main sequence (ZAMS); subgiant branch (SGB); red giant branch (RGB); core helium flash (HeF); horizontal branch (HB); early asymptotic giant branch (E-AGB); thermally pulsing asymptotic giant

(TP-AGB); post asymptotic giant branch (P-AGB); planetary nebula nucleus (PNN); carbon–oxygen white dwarf (CO-WD).

Metal-poor stars in the initial mass range of $0.4 M_{\odot} \lesssim M \lesssim 2 M_{\odot}$ appear during core helium burning in a region marked by the horizontal dashed line in part (a), depending on the mass loss during the RGB phase. The two dashed diagonal lines indicate the instability strip. In part (b) the core burning phases are labeled by the nuclear fuel: hydrogen (H), helium (He), carbon (C), and so on. The onset of carbon burning is marked by the full circle. Note the vastly different luminosity scale in parts (a) and (b). See the text.

ignites quiescently in the center. Subsequently, these stars make excursions to the left (toward higher temperatures) in the Hertzsprung–Russell diagram and some of them are liable to pass into the instability strip. The observational counterparts of these variable stars are called *classical Cepheids*. They are important for establishing a cosmic distance scale since their observed pulsation period is correlated with their luminosity.

Stars with initial masses of $M \gtrsim 4 M_{\odot}$ experience an additional episode of mixing. Following core helium exhaustion in the core, the structural readjustment to helium shell burning results in a strong expansion, such that the hydrogen burning shell is extinguished as the star begins to ascend the early asymptotic giant branch (E-AGB). At this time the inner edge of the convective envelope penetrates the dormant hydrogen shell, and the products of hydrogen burning are mixed to the surface. This process is referred to as the “second dredge-up.” Afterward, the hydrogen shell reignites and the star continues to evolve up the asymptotic giant branch (AGB).

The evolution of stars in the initial mass range of $9 M_{\odot} \lesssim M \lesssim 11 M_{\odot}$ is more complicated and less established at present. Models predict a number of important differences compared to the evolution of lower mass stars. We will discuss the evolution of a $10 M_{\odot}$ star with initial solar composition as an example (Ritossa, García-Berro and Iben 1996). The star starts out by burning hydrogen in the core via the CNO cycles for about 10 million years. Following the exhaustion of hydrogen in its center, the star evolves toward the red giant branch where eventually the first dredge-up event occurs. Helium burning starts in the core under nondegenerate conditions and lasts for about 270,000 years. After helium exhaustion, the core contracts and heats up, and the outer layers of the star expand. Thereafter, the hydrogen burning shell extinguishes, while helium continues to burn in a shell surrounding a partially electron degenerate carbon–oxygen core. Eventually, the core becomes sufficiently hot for the fusion of carbon nuclei (*carbon burning*). When carbon ignites, the star enters the super asymptotic giant branch (SAGB). Carbon burning starts with a thermonuclear runaway (*carbon flash*) and the energy generation rate from carbon fusion increases greatly. The energy release causes the overlying layers to expand, giving rise to a reduction in the helium shell burning energy generation rate. After a relaxation period, the helium burning shell returns to its prior energy output. Several of these flashes occur over the carbon burning lifetime, which lasts for about 20,000 years. When carbon is exhausted in the center, the electron degenerate core consists mainly of oxygen and neon. After carbon burning extinguishes, the second dredge-up event occurs. Subsequently, the dormant hydrogen shell on top of the helium burning shell is reactivated and a complicated interplay between these two burning shells gives rise to thermal pulses which are driven by helium shell flashes. During this time, the third dredge-up event occurs. Eventually, the hydrogen-rich surface

is removed by a strong stellar wind and the star becomes the central object of a planetary nebula. It ends its existence as a oxygen–neon white dwarf with a mass of $\approx 1.2 M_{\odot}$.

Initial mass of $M \gtrsim 11 M_{\odot}$

The evolution of stars in this mass range is in many ways fundamentally different compared to our earlier discussion. Schematic evolutionary tracks for $13 M_{\odot}$, $15 M_{\odot}$, $20 M_{\odot}$, and $25 M_{\odot}$ stars are shown in Fig. 1.5b. The case of a $25 M_{\odot}$ star with initial solar composition will be discussed in the following as an example (Chieffi, Limongi and Straniero 1998; Limongi, Straniero and Chieffi 2000; Woosley, Heger and Weaver 2002). The total life of such a massive stars is relatively short and amounts only to ≈ 7 My. The star spends 90% of this time on the main-sequence burning hydrogen to helium via the CNO cycles in the core. When the hydrogen in the center is exhausted, hydrogen burning continues in a shell. The core contracts and heats up until helium is ignited. This new source of nuclear energy heats the overlying hydrogen shell and the outer layers of the star expand greatly. The star becomes a supergiant. These stars show up in the Hertzsprung–Russell diagram at the highest observed luminosities. Examples are Rigel (blue supergiant) and Betelgeuse (red supergiant) in the constellation Orion.

Core helium burning lasts for about 800,000 years and some of the heavy nuclides with masses of $A > 60$ are synthesized during this stage via neutron captures (s-process; Section 5.6.1). When helium is exhausted in the center, helium burning continues in a shell located beneath the hydrogen burning shell. Eventually, carbon burning starts in the core. These burning stages have already been discussed above.

Stars with initial masses exceeding $\approx 11 M_{\odot}$ are capable of igniting successive burning stages in their cores using the ashes of the previous core burning stage as fuel. Three distinct burning stages follow carbon burning. They are referred to as *neon burning*, *oxygen burning*, and *silicon burning*, and will be discussed in detail in Section 5.5. There is a fundamental difference between the initial and the advanced burning stages in the manner by which the nuclear energy generated in the stellar interior is transformed and radiated from the surface. For hydrogen and helium burning, nuclear energy is almost exclusively converted to light. During the advanced burning stages energy is almost entirely radiated as neutrino–antineutrino pairs and the light radiated from the star’s surface represents only a very small fraction of the total energy release. Since the neutrino losses increase dramatically during the advanced burning stages and because the nuclear burning lifetime scales inversely with the total luminosity, the evolution of the star rapidly accelerates. For example, silicon burning will last for only about 1 day (Chapter 5). Since the advanced burning stages transpire very quickly, the envelope has insufficient time to re-

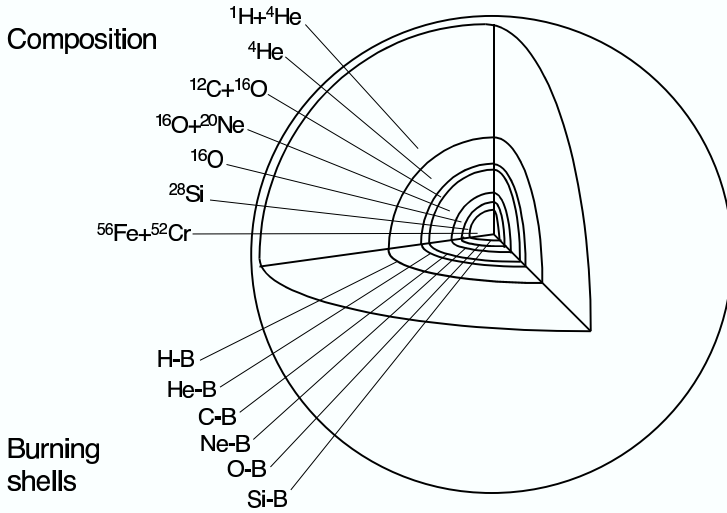


Fig. 1.6 Schematic structure of a presupernova star (not to scale). The upper-left side shows the one or two most abundant nuclear species in each region (according to Limongi, Straniero and Chieffi 2000). Nuclear reactions are very temperature dependent. Thus the nuclear burning takes

place in relatively thin shells at the interface between layers of different composition. The nuclear burning shells are labeled on the lower-left side; for example, “H-B” stands for hydrogen burning. This model is sometimes referred to as the “onion shell structure” of a massive star.

act to the structural changes in the stellar interior. Thus, from carbon burning onward, the star will no longer move in the Hertzsprung–Russell diagram, but remains at the position indicated by the solid circle in Fig. 1.5b. Furthermore, since the star spends most of its life burning either hydrogen or helium in the core, these are typically the only phases that we can observe.

The approximate structure of the massive star after the silicon has been exhausted in the core is shown in Fig. 1.6. The star consists now of several layers of different composition that are separated by thin nuclear burning shells. The details of the nucleosynthesis are complicated and will be discussed in Chapter 5. It is sufficient to mention at this point that the heaviest and most stable nuclei (that is, the iron peak nuclei; Section 1.3) are found in the core. In fact, the most abundant nuclide in the core is ${}^{56}\text{Fe}$. It should also be noted that the luminosity during the red giant phase is so large that the star undergoes a significant mass loss. The effect is more pronounced for stars with $M \gtrsim 30\text{--}35 M_{\odot}$ that lose eventually most of their hydrogen envelope. The observational counterparts of such stars are the hot and massive *Wolf–Rayet stars*, which have been observed to lose mass at a rate of $\approx 10^{-5} M_{\odot}$ per year at stellar wind speeds of ≈ 2000 km/s. An image of a Wolf–Rayet star is shown in color Fig. 5 on page 635.

The electron degenerate stellar core has at this point no other sources of nuclear energy to its disposal and grows in mass as the overlying burning shells contribute nuclear ashes. When the mass of the core exceeds the Chandrasekhar limit ($\approx 1.4 M_{\odot}$), the electron degeneracy pressure is unable to counteract gravity, and the core collapses. The core collapse is accelerated by two important effects. First, as the electron density increases, electrons capture onto iron peak nuclei (Section 1.8.4). This removes electrons that were contributing to the pressure. Second, at temperatures of ≈ 5 GK, the thermal radiation becomes sufficiently energetic and intense that the iron peak nuclei are photodisintegrated into lighter and less stable nuclei. This process removes energy that could have provided pressure. At this stage the core of the star is essentially collapsing in free fall. When the density reaches values on the order of the nuclear density ($\approx 10^{14}$ g/cm³), the nuclei and free nucleons begin to feel the short-range nuclear force, which is repulsive at very short distances. The inner collapsing core reaches high inward velocities and overshoots the nuclear density. The nuclear potential acts as a stiff spring that stores energy in the compressive phase until it rebounds. The rebounding part of the core encounters infalling matter and thus gives rise to an outward moving shock wave. The very hot and dense inner core has become a proto-neutron star with a mass of $\approx 1.5 M_{\odot}$.

While the shock wave moves outward through the outer core region, it loses energy by photodisintegrating the iron peak nuclei. Furthermore, energy is removed from the shock wave by the emission of neutrinos. It takes about 1 s after core collapse, and about 10 ms after the core has bounced, for the shock wave to reach the outer edge of the core. At this time the shock wave has lost all of its kinetic energy and it stalls. How exactly the shock is revived and how it will ultimately propagate through the stellar layers beyond the iron core and disrupt the star in a core collapse supernova explosion is still unknown. The stalled shock wave is thought to be revived by the neutrinos and antineutrinos that emerge from the hot and dense proto-neutron star, a fraction of which is absorbed by protons and neutrons behind the shock (Bethe and Wilson 1985).

Once the shock wave is revived by the neutrino energy deposition, it propagates outward beyond the iron core and compresses and heats each of the overlying shells of the star. Some of the shells experience, after hydrostatic burning prior to core collapse, another episode of nucleosynthesis which proceeds on timescales of a few seconds and is called *explosive nuclear burning*. The silicon (^{28}Si) and oxygen (^{16}O) in the first layers that the shock wave encounters (Fig. 1.6) are quickly converted to iron peak nuclei at high temperatures (≈ 5 GK). It will be shown in Section 5.5.5 that under such conditions the most abundant product nuclide originating from these layers is $^{56}_{28}\text{Ni}_{28}$. By the time the shock wave reaches the other layers of the star, the temperatures achieved are much smaller and hence these are ejected into space with less